Using the Fuzzy Spatial Relation "Between" to Segment the Heart in Computerized Tomography Images

Antonio Moreno*, Isabelle Bloch†, Celina Maki Takemura‡, Olivier Colliot§ and Oscar Camara¶

*,† *GET-ENST, TSI Department*
CNRS UMR 5141 LTCI Paris, France
**Antonio.Moreno@enst.fr*
†*Isabelle.Bloch@enst.fr*
‡ *Department of Computer Science*
Institute of Mathematics and Statistics (IME)
University of São Paulo (USP), São Paulo, Brazil
§ *Cognitive Neuroscience and Brain Imaging Laboratory*
CNRS UPR 640-LENA, Université Pierre et Marie Curie — Paris 6
Hôpital de la Pitié-Salpétrière, Paris, France
¶ *Computational Imaging Lab, Department of Information and Communication Technologies, Universitat Pompeu Fabra*
Passeig Circumval-lació 8, 08003 Barcelona, Spain

Abstract

Segmenting the heart in medical images is a challenging and important task for many applications. Most heart segmentation methods proposed in the literature deal with cardiac internal structures, but there is a real interest in segmenting the heart as a whole. In this paper, we address this problem and propose an automatic method, based on the modeling of spatial relations of

*A. Moreno is currently at INSERM U.562 — Cognitive Neuroimaging Unit, CEA/SAC/DSV/I2BM/NeuroSpin, Bâtiment 145, Point Courrier 156, F-91191 Gif-sur-Yvette CEDEX, France.

the heart with the lungs. The main a priori anatomical knowledge we use in this work is expressed by the spatial relation "the heart is between the lungs" and we propose a fuzzy representation of this anatomical knowledge, which then drives the segmentation process.

1. Introduction

Segmenting the heart in medical images such as noncontrast computerized tomography (CT) images is a challenging task due to their low contrast and the similar gray-level values of the surrounding structures (liver, tumors). Many clinical applications could benefit from a reliable heart segmentation procedure, such as the study of cancer in the thoracic region or other cardiac and vascular diseases. The delineation of the heart is important in oncological applications such as dose estimation in radiotherapy: it may be used in treatment planning in order to define a security margin around this organ to prevent it from being irradiated. It can also be useful as a preliminary step for registration of multimodal images.

Most heart segmentation methods proposed in the literature deal with segmentation of internal structures (in particular the left ventricle)[1,2] and are focused on MRI modality or ultrasound but rarely on CT. However, in particular for the aforementioned applications (where CT is one of the most common anatomical imaging modalities), there is also a need to segment the heart as a whole in order to distinguish its limits and the separations with surrounding structures (as the liver). Among the existing methods for segmenting the heart as a whole, Gregson[3] works on MR images where he manually selects a 2D slice containing the heart and then uses a hierarchical algorithm to segment other structures in this slice (torso, lungs, background). Once the heart is recognized in the selected slice, the segmentation is propagated to adjacent slices. Lelieveldt *et al.*[4] proposed another method based on a fuzzy atlas of thoracic structures. Their method is applied on MR data and the fuzzy model must be built beforehand, which is a strong limitation, in particular for the segmentation of pathological images that may have a different structural configuration than the ones used for the atlas construction. The segmentation method proposed by Jolly,[5] developed to segment the left ventricle in 2D MR slices, has been extended to CT with minimal adjustments. Her method proceeds in two steps. First, a global localization step roughly localizes the left ventricle and then a local deformation step

combines EM-based (Expectation-Maximization) region segmentation and Dijkstra active contours. This method furnishes very satisfactory results for high-resolution contrast CT images. The work of Funka-Lea *et al.*[6] deals with the segmentation of the heart as a whole in CT. Their goal is to isolate the outer surface of the entire heart in order to easily visualize the coronary vessels. They make use of graph-cuts for the segmentation. Their method is fast and robust for contrast CT studies with sub-millimeter resolution where the brightest regions are bone and blood. The recent work of Ecabert *et al.*[7] describes a multi-compartment mesh of both atria, both ventricles, the myocardium around the left ventricle and the trunks of the great vessels and it is adapted to an image volume. The adaptation is performed in a coarse-to-fine manner by progressively relaxing constraints on the degrees of freedom of the allowed deformations. Their method is largely validated and it furnishes very satisfactory results. However, these methods are not directly applicable to noncontrast and low resolution 3D CT images and major adaptations and extensions would be needed.

In addition to their low contrast and the similar gray-level values of the surrounding structures, noncontrast CT images present specific difficulties for the segmentation of the heart due to their low resolution (compared to existing submillimetric CT data) and their anisotropy. For these reasons, there exist few methods for the segmentation of the heart for noncontrast CT images and the existing methods for other modalities cannot deal with this type of images.

In this paper, we propose an automatic method based on the modeling of spatial relations of the heart with surrounding structures. In this particular case, the main a priori anatomical knowledge we use is expressed by the spatial relation "the heart is between the lungs". Several definitions of this knowledge are presented and we discuss which one is more adapted to our problem. This work extends a preliminary version.[8] Since the segmentation of the lungs is generally straightforward in CT scans due to their high contrast with respect to surrounding structures, we first segment them in order to obtain the region of interest (ROI) of the heart. Then we add the anatomical knowledge to the evolution of a deformable model to precisely segment the heart.

In Sec. 2, we introduce the basis of our approach: the spatial relation "between". In Sec. 3, the main steps of our approach are detailed.

Next, in Sec. 4 some results are shown and discussed. Finally, in Sec. 5 we conclude and evoke some future work.

2. The Spatial Relation "Between"

Usual anatomical descriptions of the heart include a common statement: "the heart is between the lungs". Our method relies on modeling this statement.

A complete study of the spatial relation "between" has been made by Bloch *et al.*:[9] different definitions of this spatial relation were proposed, compared and discussed according to different types of situations. The main ones are discussed here in light of the specificities of the addressed problem. We restrict ourselves to definitions designed for objects having similar spatial extensions.

Crisp Definitions — The most intuitive crisp definition is based on the convex hull of the union of the objects. However this approach is not appropriate to find the ROI of the heart because some parts of the heart are not included in this convex hull as shown in Fig. 1. A more flexible definition is therefore required. This is a strong argument in favor of one of the following fuzzy definitions.

Fuzzy Dilations — The region between A_1 and A_2 is defined as a fuzzy set in the image domain. Our problem involves nonconvex shapes (the lungs) which have important concavities facing each other (the cavity of the heart). For this reason, the fuzzy directional dilation definitions of the relation "between" are adapted to this case. The simplest definition is:

$$\beta_{FDil1}(A_1, A_2) = D_{\nu_2}(A_1) \cap D_{\nu_1}(A_2) \cap A_1^C \cap A_2^C, \qquad (1)$$

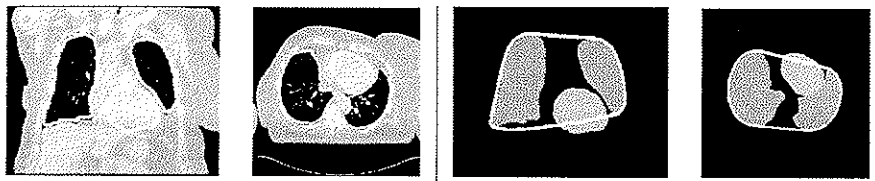

(a) (b) (c) (d)

Fig. 1. Coronal (a, c) and axial (b, d) views of an example of the segmentation of the lungs and the heart. The contours of these organs are superimposed on the original image (on the left) and the convex hull is superimposed on the segmented lungs and heart (on the right): Some parts of the heart are not contained in this region.

where A_1 and A_2 represent the objects (the lungs in our case), A^C represents the (fuzzy) complementation of A and $D_{\nu_i}(A_j)$, $i, j \in \{1, 2\}$, is the fuzzy dilation of A_j with the fuzzy structuring element ν_i: $D_\nu(\mu)(x) = \sup_y t[\mu(y), \nu(x - y)]$ where μ denotes the (fuzzy) set to be dilated, ν the structuring element, t a t-norm and x and y points of space.[10]

The structuring elements are derived from the angle histogram between the objects.[11] For instance, if object A_2 is mainly to the right of object A_1, then Eq. (1) defines the region which is both to the right of A_1 and to the left of A_2 (excluding A_1 and A_2). This definition is illustrated in Fig. 2(a).

Another definition of "between", which removes the concavities of the objects which are not facing each other, is:

$$\begin{aligned}\beta_{FDil2}(A_1, A_2) = {} & D_{\nu_2}(A_1) \cap D_{\nu_1}(A_2) \cap A_1^C \cap A_2^C \\ & \cap [D_{\nu_1}(A_1) \cap D_{\nu_1}(A_2)]^C \cap [D_{\nu_2}(A_1) \cap D_{\nu_2}(A_2)]^C.\end{aligned} \qquad (2)$$

In this case, if object A_2 is mainly to the right of object A_1, then Eq. (2) defines the region which is both to the right of A_1 and to the left of A_2 (excluding A_1 and A_2), but which is not to the left of both A_1 and A_2 nor to the right of both. Figure 2(b) shows the region between the lungs obtained with this definition.

Admissible segments — The notion of visibility plays an important role in the definition of "between" as illustrated by Bloch

(a) (b) (c)

Fig. 2. Fuzzy regions between the lungs, superimposed on an axial slice of the segmented lungs (in gray and dark gray): (a) β_{FDil1}, (b) β_{FDil2} and (c) β_{FVisib}. Their membership values vary from 0 (white) to 1 (black). It can be observed that β_{FDil1} does not remove the concavities of the objects which are not facing each other.

et al.[9] The visible points are those which belong to admissible segments[a] and the region $\beta_{Adm}(A_1, A_2)$ between A_1 and A_2 can then be defined as the union of admissible segments. However, the definition of admissible segments may be too strict in some cases, in a similar manner as the convex hull definition (see Fig. 1). For this reason, the notion of approximate (or fuzzy) visibility has been introduced. Thus, a segment $]a_1, P]$ with $a_1 \in A_1$ (respectively $[P, a_2[$ with $a_2 \in A_2$) is said semi-admissible if it is included in $A_1^C \cap A_2^C$. At each point P of space, we compute the angle the closest to π between two semi-admissible segments from P to A_1 and A_2 respectively. This is formally defined as:

$$\begin{aligned}\theta_{\min}(P) &= \min\{|\pi - \theta|, \theta \\ &= \angle([a_1, P], [P, a_2]),]a_1, P] \text{ and } [P, a_2[\text{ semi-admissible}\}.\end{aligned} \tag{3}$$

The region between A_1 and A_2 is then defined as the fuzzy region of space with membership function:

$$\beta_{FVisib}(A_1, A_2)(P) = f(\theta_{\min}(P)), \tag{4}$$

where f is a function from $[0, \pi]$ to $[0, 1]$ such that $f(0) = 1$, f is decreasing, and becomes 0 at the largest acceptable distance to π (this value can be tuned according to the context). The result obtained with this definition is illustrated in Fig. 2(c).

Selected Definition — In order to decide which definitions better match our problem, we have compared them with respect to two criteria:

(1) *Concavities.* The fuzzy dilation definition β_{FDil1} does not remove the concavities of the objects which are not facing each other (see Fig. 2). However, β_{FDil2} and β_{FVisib} do. Therefore, we prefer to use β_{FDil2} or β_{FVisib}, in order not to include the small concavities of the lungs which do not correspond to the heart but to vessels and bronchi.
(2) *Complexity.* For the methods based on fuzzy dilations, the complexity is $O(NN_\nu)$ where N denotes the cardinality of the bounded space in which the computation is performed (the image) and N_ν is the cardinality of the support of the structuring element used in the fuzzy dilations. The morphological approach additionally requires the computation of the angle histogram which has a complexity of $O(N_1 N_2)$, where N_i denotes the cardinality of A_i. The computation of $\beta_{Adm}(A_1, A_2)$ for the admissible segments method is of the order of $N_1 N_2 \sqrt{N}$. Finally, the fuzzy visibility approach has a complexity of $O(NN_1N_2)$.

[a] A segment $]x_1, x_2[$, with x_1 in A_1 and x_2 in A_2, is said to be admissible if it is included in $A_1^C \cap A_2^C$.

As β_{FDil2} and β_{FVisib} furnish comparable results with respect to concavities, we prefer β_{FDil2} due to its lower complexity. In order to reduce computing time, images can be under-sampled to obtain the region between the lungs, since a very precise result is not necessary at this stage. In this case, the small concavities may be removed by the under-sampling and therefore the differences between β_{FDil1} and β_{FDil2} are notably reduced.

Finally, we define: $\beta_{btw}(A_1, A_2) = \beta_{FDil2}(A_1, A_2)$. The interest of the selected fuzzy definitions is that the between region extends smoothly outside the convex hull of the union of both objects which is a required feature for our application (see Fig. 1).

3. Using "Between" to Segment the Heart

The main feature of our approach is to include the anatomical knowledge "the heart is between the lungs" in the segmentation process of the heart in CT images. This knowledge is modeled by the spatial relation "between" as explained in Sec. 2.

As detailed in our previous work,[8] we proceed in two steps:

(1) we select the region of interest (ROI) by combining the spatial relation "between" and the distance to the lungs;
(2) we introduce the spatial relation "between" in the evolution scheme of a deformable model to find the boundaries of the heart.

In our approach, we lean on the segmentation of the lungs, which relies on previous work.[12] An example of the segmentation of the lungs is illustrated in Fig. 1.

3.1. *Definition of the region of interest*

First, we want to find the region of interest where the heart is contained. The heart is in the space between the lungs, more precisely,

in the widest part of this region, where the lungs are the farthest from each other. For this reason, we propose to combine the spatial relation "between" and the distance to the lungs in order to find the ROI.

In 2D, as explained by Gregson,[3] the maximum of the distance function to the lungs (on a previously selected slice containing the heart) is a good candidate to be the center of a disk containing this organ (the radius of this disk being 110% of the value of the distance at the center point).

We extend this idea to 3D and improve it in order to avoid failure cases by combining the distance to the lungs with the spatial relation "between". This distance function is computed using a chamfer algorithm.[13] However, the maximum of the distance to the lungs is not necessarily contained inside the heart.

To solve this problem, we combine the distance with the spatial relation "between". The goal is to find a robust candidate to be the center of a sphere that will contain the whole heart. Obviously this point (as it is inside the heart) will be in the region between the lungs with a high value of the membership function β_{btw} (see Fig. 3(a)), and it should be one of the points with a maximum distance to both lungs. The normalized distance function can be interpreted as a fuzzy set which represents the region "far from the lungs". Its membership function β_{ffl} is shown in Fig. 3(b).

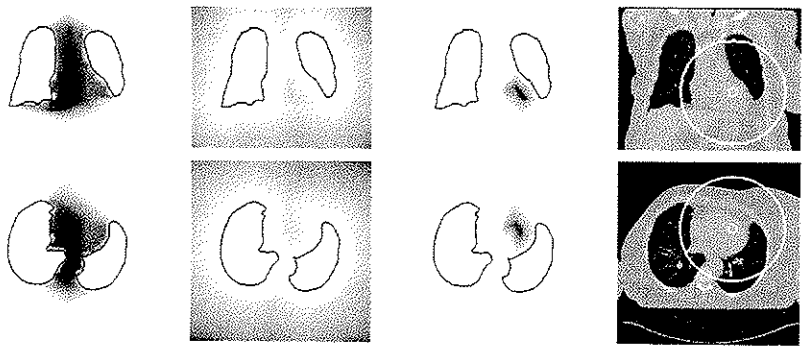

(a) (b) (c) (d)

Fig. 3. (a) The spatial relation "between" β_{btw} calculated with Eq. (2). (b) The distance map to the lungs β_{ffl} and (c) the conjunctive fusion of both β_R. (d) Image shows the obtained ROI of the heart and the initial contour of the deformable model superimposed on the original image. Coronal views are in the top row and axial views in the bottom one.

Thus, the algorithm to find the center of the heart has two different steps:

(1) *Combination of anatomical knowledge.* Let us denote by β_R the fusion of β_{btw} and β_{ffl}:

$$\beta_R(x) = \beta_{btw}(x) \cdot \beta_{ffl}(x). \tag{5}$$

This is the combination of the distance to the lungs and the "between" function defined by Eq. (2). This combination is done with a conjunctive fusion with the t-norm "product", which means that the points with higher values will fulfill both spatial constraints. The result of this combination is shown in Fig. 3(c).

(2) *Calculation of the sphere-ROI.* The center of the sphere is defined as the point having the maximum value in the previous result. The radius is simply defined as 110% of the value of the distance at this point.

This stage provides a restricted ROI for the heart (not too many surrounding structures included) and it is robust as it uses two stable characteristics of the center of the heart. The resulting ROI is used to constrain a deformable model to remain inside this region and to define the initialization for the deformable model as a small sphere centered in this ROI (see Fig. 3(d)).

3.2. *Segmentation using a deformable model*

Once we have selected the region of interest and the initialization, we use a deformable model to segment precisely the heart. Deformable models were introduced by Kass *et al.*[14] and are often used for segmentation in image processing. They consist in defining an initial surface (in 3D) that evolves under the effect of some forces towards a final state that should correspond to the object we want to segment. The evolution of the deformable surface $\mathbf{X}$ can be described using a dynamic force formulation and written as follows:

$$\gamma \frac{\partial \mathbf{X}}{\partial t} = \mathbf{F}_{int}(\mathbf{X}) + \mathbf{F}_{ext}(\mathbf{X}), \tag{6}$$

where $\mathbf{F}_{int}$ is the *internal* force related to the physical properties or constraints of the model that specifies the regularity of the surface,[14] and $\mathbf{F}_{ext}$ is the *external* force that drives the surface towards the desired features in the image (in general image edges) and sometimes

includes forces interactively introduced by the user. The solution is the steady state of the previous equation.

The external force can be defined with the Gradient Vector Flow (GVF)[15] as also used in previous work.[12,16,17] The GVF defines a vector field towards the previously calculated contours of the image (the edge map). As proposed in our previous work[18] the external force can also include spatial relations in order to constraint the segmented object to stay in a region where given spatial relations are satisfied.

We introduce the spatial relation "between" combined with "far from the lungs" in the external force $\mathbf{F}_{ext}$ (Eq. (6)). Thus, this force describes both edge information (GVF) and structural constraints:

$$\mathbf{F}_{ext} = \lambda \mathbf{F}_{gvf} + (1 - \lambda) \mathbf{F}_R, \tag{7}$$

where $\mathbf{F}_{gvf}$ is a classical data term that drives the model towards the edges,[15] $\mathbf{F}_R$ is a force associated to the spatial relations and λ is a weighting coefficient. The force $\mathbf{F}_R$ must constrain the model to evolve towards the regions with high values of $\beta'_R = 1 - \beta_R$, i.e. regions closer to the lungs and "less between" them than the center. When the relation β'_R is completely satisfied (not between and inside the lungs), the model should only be driven by edge information ($\mathbf{F}_{gvf}$) and we should have $\mathbf{F}_R = 0$ if $\beta'_R = 1$. This illustrates an important advantage of using fuzzy spatial relations to guide the model, as we can define a vector field towards the regions where the relations are more satisfied. Several methods for external forces that fulfill these properties are described in our previous work.[18] We have chosen the one using a gradient diffusion technique because of the smoothness and the wide attraction range of the vector field calculated this way. This is detailed in our previous work.[8]

Finally, we add a pressure term to Eq. (7) in order to reinforce the effect of spatial relations and to improve convergence:

$$\mathbf{F}_{ext} = \lambda \mathbf{F}_{gvf} + (1 - \lambda) \mathbf{F}_R + \mathbf{F}_p, \tag{8}$$

where $\mathbf{F}_p$ represents a pressure force,[19] normal to the surface and of module $w_p(x)$ defined as:

$$w_p(x) = k \beta_R, \tag{9}$$

where k is a constant. This means that the pressure force is stronger at the points between the lungs which are the farthest from them (where β_R takes higher values), and it decreases when getting closer to them (where β_R takes lower values because the chosen spatial relations are less fulfilled).

4. Results and Discussion

We have applied our algorithm on 10 different cases of CT images coded on 8 bits, with sizes $512 \times 512 \times Z$ voxels with Z varying from 63 to 122 and resolutions typically around 2 mm $\times$ 2 mm $\times$ dz mm for the three directions of the space (X, Y and Z respectively), with dz varying from 4.5 to 7.5 mm.

In our experiments, we have used the following parameters:

- The initial mesh for the deformable model is a sphere with a small enough radius (10 mm) to ensure that the starting surface is completely contained inside the contours of the heart.
- The value of λ in Eq. (8) is 0.7, which gives a more important weight to the GVF force. Obviously, the weight of $\mathbf{F}_{gvf}$ should be more important because it guides the deformable model precisely towards the contours, whereas $\mathbf{F}_R$ represents a more general evolution. However, the spatial relation force remains necessary for the evolution of the deformable model.
- The constant k for the pressure force weight in Eq. (9) is $k = 0.05$. This constant balances the pressure force in order to prevent the deformable model from inflating too much or too little.
- The number of iterations for the evolution of the deformable model (simplex mesh) is 10000, which is sufficient for convergence of the model. The internal force coefficients are $\alpha = 0.2$ and $\beta = 0.1$ which provide a good trade-off between tension and rigidity.

These parameters were set experimentally. The algorithm has been applied to the 10 different cases obtaining good results. The comparison with manual segmentations provides mean distances varying from 3.9 to 9.3 mm, which is perfectly acceptable with voxel resolutions in Z between 4.5 and 7.5 mm. As explained and illustrated in our previous work,[8] all the terms in Eq. (8) are necessary to obtain correct results, and the addition of the spatial relations significantly improves the accuracy and the robustness of the heart segmentation algorithm. Some results for different patients are illustrated in Fig. 4.

Figure 5 shows some results of the segmentation of the heart with different definitions of the spatial relation "the heart is between

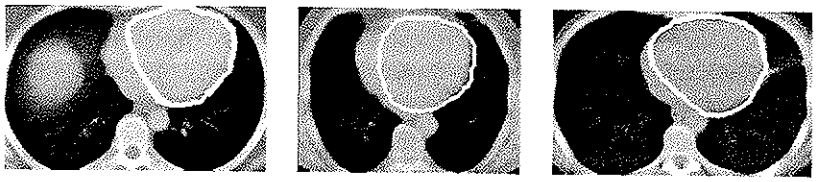

Fig. 4. Axial views of some results of the automatic segmentation of the heart using our method for three other patients.

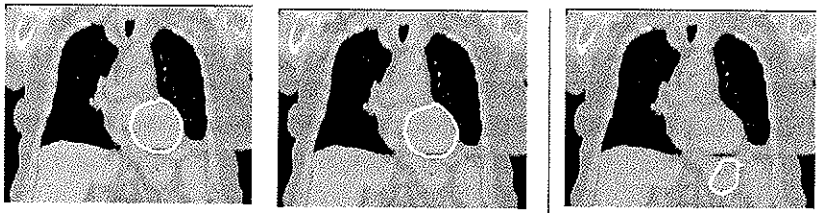

(a) (b) (c)

Fig. 5. Coronal views of some results of heart segmentation with different definitions of the spatial relation "between": (a) using β_{FDil1} and (b) using β_{FDil2}. A similar result is obtained with β_{FVisib}. (c) Result of heart segmentation using β_{FVisib}, when the acceptable distance to π is not tuned correctly.

the lungs". The results obtained using any of the fuzzy definitions β_{FDil1}, β_{FDil2} or β_{FVisib} are very satisfactory and very similar in all cases.

For the use of β_{FVisib}, however, the acceptable distance to π (i.e. the shape of the function f in Eq. (4)) has to be tuned appropriately in order to obtain a correct result. Otherwise, incorrect results of heart segmentation can be obtained as illustrated in Fig. 5(c). This value could vary for different anatomies. The definitions of "between" that use fuzzy dilations do not have this limitation as the shape of the structuring element is computed from the angle histogram, which is adapted automatically to each particular case.

5. Conclusion and Future Work

We propose an approach that uses fuzzy structural knowledge coming from the spatial relations "between the lungs" and "far from the lungs" to segment the heart in CT images in a robust way. First, spatial relations are used to define the region of interest of the heart and then we derive, from the fuzzy sets representing the spatial relations, a new external force that is introduced in the evolution scheme of a deformable model. In this paper, several definitions of the spatial relation "between" are presented. The discussion of the results shows that a fuzzy dilation definition with removes concavities is best adapted to our problem. The proposed method substantially improves the segmentation of the heart compared to classical approaches which use only a pressure force and GVF, and it avoids the surrounding structures to be included in the final segmentation of the heart. The results still have to be validated on larger databases with medical experts. However, preliminary quantitative results based on the comparison with manual segmentations performed by an expert show a strong agreement between the manual segmentations and the ones obtained by our approach. This confirms the potential of the proposed method.

Future work will aim at applying our algorithm to other imaging modalities such as positron emission tomography (PET) images.

Further applications include the use of the segmentation of the heart in registration algorithms based on structures[20] and, subsequently, in radiotherapy planning procedures.

Acknowledgments

The authors would like to thank Liège, Lille, Louisville and Val de Grâce Hospitals for the images and the members of Segami Corporation for their contribution to this project. This work was partially supported by the French Ministry of Research, by the CAPES (BEX3402/04-5) and by a "ParisTech/Région Ile-de-France" Fellowship.

References

1. H. C. van Assen, M. G. Danilouchkine, A. F. Frangi, S. Ordás, J. J. M. Westenberg, J. H. C. Reiber and B. P. F. Lelieveldt, SPASM: A 3D-ASM for segmentation of sparse and arbitrarily oriented cardiac MRI data. *Medical Image Analysis*, **10**(2), 286–303 (2006).
2. J. S. Suri, Computer vision, pattern recognition and image processing in left ventricle segmentation: The last 50 years. *Pattern Analysis & Applications*, **3**(3), 209–242 (2000).
3. P. H. Gregson, Automatic segmentation of the heart in 3D MR images. *Canadian Conference on Electrical and Computer Engineering*, **2**, 584–587 (1994).

4. B. P. F. Lelieveldt, R. J. van der Geest, M. R. Rezaee, J. G. Bosch and J. H. C. Reiber, Anatomical model matching with fuzzy implicit surfaces for segmentation of thoracic volume scans. *IEEE Transactions on Medical Imaging*, **18**(3), 218–230 (1999).
5. M.-P. Jolly, Automatic segmentation of the left ventricle in cardiac MR and CT images. *International Journal of Computer Vision*, **70**(2), 151–163 (2006).
6. G. Funka-Lea, Y. Boykov, C. Florin, M.-P. Jolly, R. Moreau-Gobard, R. Ramaraj and D. Rinck, Automatic heart isolation for CT coronary visualization using graph-cuts. *IEEE International Symposium on Biomedical Imaging (ISBI)*, Arlington, Virginia, USA, pp. 614–617 (2006).
7. O. Ecabert, J. Peters, M. J. Walker, J. von Berg, C. Lorenz, M. Vembar, M. E. Olszewski and J. Weese, Automatic whole heart segmentation in CT images: Method and validation. (eds.) J. Pluim and J. Reinhardt, *SPIE Medical Imaging*, San Diego, California, USA **6512** (2007).
8. A. Moreno, C. M. Takemura, O. Colliot, O. Camara and I. Bloch, Heart segmentation in medical images using the fuzzy spatial relation "Between". *Information Processing and Management of Uncertainty in Knowledge-Based Systems (IPMU)*, Paris, France, pp. 2052–2059 (2006).
9. I. Bloch, O. Colliot and R. M. Cesar, On the ternary spatial relation "Between". *IEEE Transactions on Systems, Man, and Cybernetics SMC-B*, **36**(2), 312–327 (2006).
10. I. Bloch and H. Maître, Fuzzy mathematical morphologies: A comparative study. *Pattern Recognition*, **28**(9), 1341–1387 (1995).
11. K. Miyajima and A. Ralescu, Spatial organization in 2D segmented images: Representation and recognition of primitive spatial relations. *Fuzzy Sets and Systems*, **65**(2/3), 225–236 (1994).
12. O. Camara, O. Colliot and I. Bloch, Computational modeling of thoracic and abdominal anatomy using spatial relationships for image segmentation. *Real-Time Imaging*, **10**(4), 263–273 (2004).
13. G. Borgefors, Distance transformations in digital images. *Computer Vision, Graphics, and Image Processing (CVGIP)*, **34**(3), 344–371 (1986).
14. M. Kass, A. Witkin and D. Terzopoulos, Snakes: Active contour models. *International Journal of Computer Vision*, **1**(4), 321–331 (1987).
15. C. Xu and J. L. Prince, Gradient vector flow: A new external force for snakes. *IEEE Computer Society Conference on Computer Vision and Pattern Recognition*, Los Alamitos, San Juan, Puerto Rico, pp. 66–71 (1997).
16. O. Colliot, O. Camara, R. Dewynter and I. Bloch, Description of brain internal structures by means of spatial relations for MR image segmentation. *SPIE Medical Imaging*, San Diego, California, USA **5370**, pp. 444–455 (2004).
17. O. Colliot, O. Camara and I. Bloch, Integration of fuzzy spatial relations in deformable models — Application to brain MRI segmentation. *Pattern Recognition*, **39**(8), 1401–1414 (2006).
18. O. Colliot, O. Camara and I. Bloch, Integration of fuzzy structural information in deformable models. *Information Processing and Management of Uncertainty in Knowledge-Based Systems (IPMU)*, Perugia, Italy **2**, pp. 1533–1540 (2004).

19. L. D. Cohen, On active contour models and balloons. *Computer Vision, Graphics, and Image Processing: Image Understanding (CVGIP:IU)*, **53**(2), 211–218 (1991).
20. O. Camara, G. Delso, O. Colliot, A. Moreno-Ingelmo and I. Bloch, Explicit incorporation of prior anatomical information into a nonrigid registration of thoracic and abdominal CT and 18-FDG whole-body emision PET images. *IEEE Transactions on Medical Imaging*, **26**(2), 164–178 (2007).